- 1 Engineer Human Pluripotent Stem Cell-Derived Natural Killer Cells with PD-L1
- 2 Responsive Immunological Memory for Enhanced Immunotherapy Efficacy
- 4 Yun Chang,<sup>1,2</sup> Gyuhyung Jin,<sup>1,2</sup> Weichuan Luo,<sup>3</sup> Qian Luo,<sup>3</sup> Juhyung Jung,<sup>1</sup> Sydney N. Hummel,<sup>1</sup>
- 5 Sandra Torregrosa-Allen<sup>2</sup>, Bennett D. Elzey<sup>2</sup>, Philip S. Low,<sup>2,3\*</sup> Xiaojun Lance Lian,<sup>4\*</sup> Xiaoping
- 6 Bao<sup>1,2\*</sup>

7

13

16

17

- 8 <sup>1</sup>Davidson School of Chemical Engineering, Purdue University, West Lafayette, IN 47907, USA.
- 9 <sup>2</sup>Purdue University Center for Cancer Research, West Lafayette, IN 47907, USA.
- <sup>3</sup>Department of Chemistry, Purdue University, West Lafayette, IN 47907, USA.
- <sup>4</sup>Departments of Biomedical Engineering, Biology, The Huck Institutes of the Life Sciences, The
- Pennsylvania State University, University Park, PA 16802, USA.
- \*Corresponding Authors: lian@psu.edu (X.L.), plow@purdue.edu (P.S.L.), bao61@purdue.edu
- 15 (X.B., lead contact).

### **ABSTRACT**

20

21

22

23

24

25

26

27

28

29

30

31

32

33

34

35

36

37

Adoptive chimeric antigen receptor (CAR)-engineered natural killer (NK) cells have shown promise in treating various cancers. However, limited immunological memory and access to sufficient numbers of allogenic donor cells have hindered their broader preclinical and clinical applications. Here, we first assessed eight different CAR constructs that use anti-PD-L1 nanobody and/or universal anti-fluorescein (FITC) single-chain variable fragment (scFv) to enhance antigen-specific proliferation and antitumor cytotoxicity of NK-92 cells against heterogenous solid tumors. We next genetically engineered human pluripotent stem cells (hPSCs) with optimized CARs and differentiated them into functional dual CAR-NK cells. The tumor microenvironment responsive anti-PD-L1 CAR effectively promoted hPSC-NK cell proliferation and cytotoxicity through antigen-dependent activation of phosphorylated STAT3 (pSTAT3) and pSTAT5 signaling pathways via intracellular truncated IL-2 receptor β-chain (ΔIL-2Rβ) and STAT3-binding tyrosine-X-X-glutamine (YXXQ) motif. Antitumor activities of PD-L1-induced memory-like hPSC-NK cells were further boosted by a FITC-folate bi-specific adapter that bridges programmable anti-FITC CAR and folate receptor alpha-expressing breast tumor cells. Collectively, our hPSC CAR-NK engineering platform is modular and could provide a realistic strategy to manufacture off-the-shelf CAR-NK cells with immunological memory-like phenotype for targeted immunotherapy.

38

39

40

## **KEY WORDS**

- 41 Natural killer cells, Human pluripotent stem cells, Immunological memory, Immunotherapy,
- 42 Chimeric antigen receptor.

43

#### INTRODUCTION

45

46

47

48

49

50

51

52

53

54

55

56

57

58

59

60

61

62

63

64

65

66

67

68

69

70

Adoptive cellular therapy (ACT)-based immunotherapy has emerged as a powerful and potentially curative therapy for the treatment of various types of cancers [1–3]. Natural killer (NK) cell-based immunotherapy [4–6] is increasingly attractive due to their innate antitumor immunity without prior sensitization and/or antigen presentation [7,8]. Furthermore, allogenic NK cells do not induce graft-versus-host disease (GvHD) after infusion, which is commonly associated with allogenic T cell transplantation [9,10]. While significant clinical benefit has been achieved in the treatment of hematologic malignancies and melanoma, the efficacy of adoptive NK cell therapy in treating solid tumors is thus far limited due in part to the failure of transferred NK cells to develop classical immunological memory [11,12], which is mainly caused by the inability of receptor genes in NK cells to undergo rearrangement and the exhaustion of NK cells under immunosuppressive tumor microenvironment [13,14]. Thus, engineering NK cells with tumor microenvironment responsive chimeric antigen receptors (CARs) holds great promise in achieving immunological memory-like activities of NK cells during tumor ablation. Specific receptor stimulation promotes significant expansion of NK cells under diseased microenvironment, and these self-renewal memory NK cells rapidly degranulate and produce cytokines upon reactivation to perform robust protective immunity [15,16]. While various tumor targeting CARs in NK cells were effectively stimulated by specific tumor antigens, their therapeutic efficacy was still limited due to the poor in vivo expansion and persistence of NK cells after infusion. The employment of cytokines, such as IL-15 [17-19], IL-18 [10,16,20-22], and IL-21 [23-25], has been widely reported to enhance in vivo persistence and/or memory of various NK cells. However, cytokine stimulation may lead to autonomous NK cell proliferation, severe adverse events, or even leukemia transformation in patients [26]. To produce superior memory-like NK cells under a robust, safe and controllable way, CAR structures should be designed to effectively and specifically recognize immunosuppressive signals in the tumor microenvironment and immediately activate intracellular proliferation signaling pathway in NK

cells [18,19], leading to tumor-responsive cellular expansion and prevention of NK cell exhaustion[27]. Among these immunosuppressive signals, programmed death-ligand 1 (PD-L1), which are expressed on various solid tumor cells and interact with PD-1 on immune cells to block immunotherapy[28-30], are widely used in CAR design since PD-L1/PD-1 blockade has achieved significant clinical benefits [31,32]. In addition to enhanced in vivo persistence, these memory-like NK cells should have excellent tumor-killing ability. CAR constructs containing transmembrane and/or co-stimulatory domains of NKG2D, 2B4, and 41BB were reported to effectively activate intracellular cytotoxicity signaling pathways in NK cells [33], but continuous exposure to antigens may cause NK cell exhaustion and prevent acquisition of memory-like phenotype in the engineered NK cells [34,35]. To avoid T cell exhaustion and cytokine storm [36–39], anti-fluorescein (FITC) single-chain variable fragment (scFv)-based CAR has been used in T cells to eradicate tumor cells only in the presence of a low molecular weight adapter [40]. These fluorescein-cancer bridging small molecules have a short circulation half-life < 90 minutes and could easily penetrate solid tumors [39]. Such a bi-specific adapter strategy may also be used to prevent NK cell exhaustion, enhance broader applicability against heterogenous solid tumors, and reduce off-target toxicity to the non-target organs. Broader application of adoptive NK cell therapy is currently hindered by the limited access to sufficient numbers of donor cells for multiple-dose transplantation [41]. Additionally, genetic modification of primary NK cells is technically challenging and laborious, leading to heterogeneous CAR-NK cells [42]. In contrast, human pluripotent stem cells (hPSCs) are capable of self-renewal and can be genetically modified to produce custom NK cells in a homogenous and clinically-scalable manner [7,33,43], rendering them as a promising platform for making realistically off-the-shelf cellular immunotherapies. In this study, we first assessed eight different CAR constructs that use anti-PD-L1 nanobody and/or universal anti-FITC scFv to enhance antigen-specific proliferation and antitumor cytotoxicity of NK cells (Fig. 1). hPSCs were then engineered with these optimized CARs and

71

72

73

74

75

76

77

78

79

80

81

82

83

84

85

86

87

88

89

90

91

92

93

94

95

differentiated into functional dual CAR-NK cells. The tumor microenvironment responsive anti-PD-L1 CAR effectively promoted hPSC-NK cell proliferation and cytotoxicity against tumor cells through antigen-dependent activation of phosphorylated STAT3 (pSTAT3) and pSTAT5 signaling pathways via intracellular truncated IL-2 receptor  $\beta$ -chain ( $\Delta$ IL-2R $\beta$ ) and STAT3-binding tyrosine-X-X-glutamine (YXXQ) motif. Antitumor activities of PD-L1-induced memory-like hPSC-NK cells were further boosted by a FITC-folate adapter that bridges programmable anti-FITC CAR and folate receptor alpha (FR $\alpha$ )-expressing breast tumor cells, but not the FR $\alpha$  rare prostate cancer cells. Notably, anti-FITC CAR is also switchable to target other tumor cells, including LNCaP using a bi-specific switch FITC-DUPA. Collectively, our hPSC CAR-NK engineering platform is designed to be modular and could provide a realistic strategy to manufacture off-the-shelf CAR-NK cells with immunological memory-like phenotype for targeted immunotherapy.

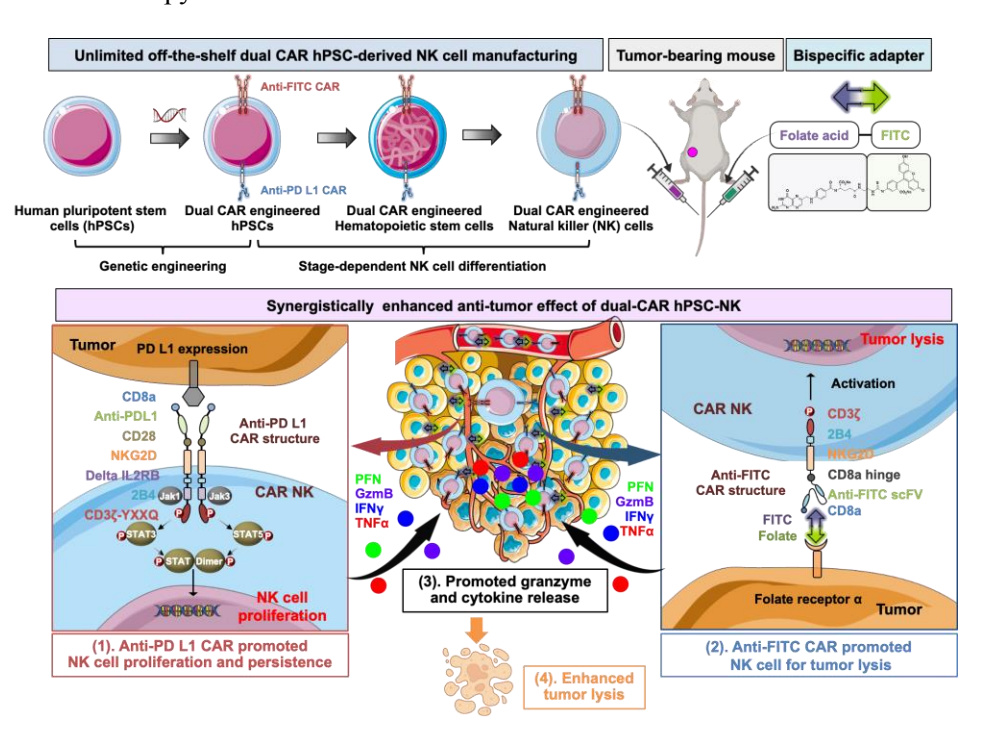


Fig. 1. Schematic of synergistically enhanced anti-tumor effect of dual CAR hPSC-NK cells.

## **RESULTS**

# Screening CAR structures with enhanced NK cell-mediated tumor-killing activities

Based on previous CAR constructs used in T and NK cells [33,39], we first designed and evaluated 8 different CAR designs optimized for antitumor cytotoxicity and proliferation in NK-92 cells (**Fig. 2A**). CAR #1 to #4 were single antigen-targeting CARs against either PD-L1 or

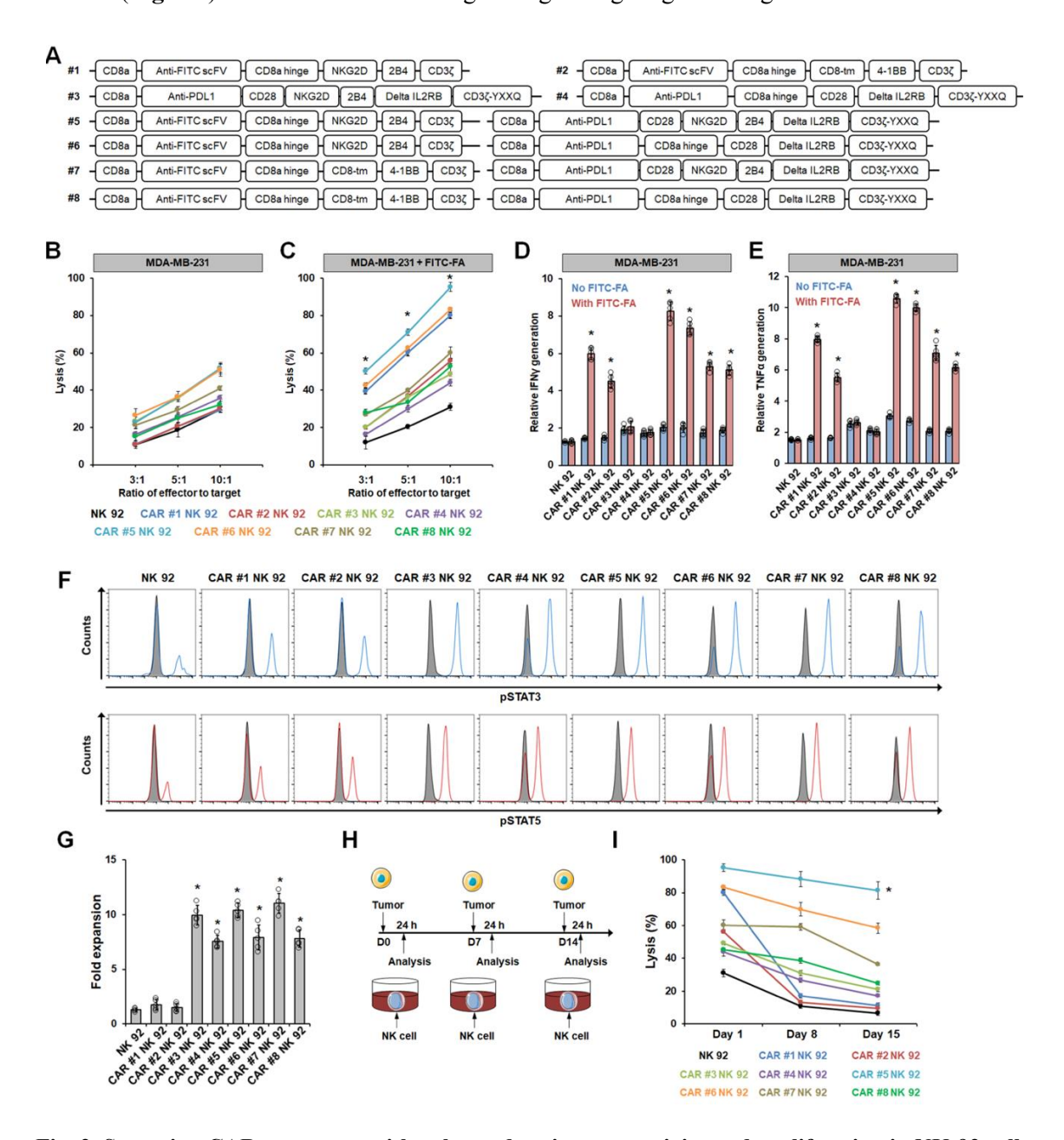


Fig. 2. Screening CAR structures with enhanced anti-tumor activity and proliferation in NK-92 cells.

(A) Schematic of various lentiviral CAR constructs. Killing of MDA-MB-231 tumor cells by indicated NK-92 cells was performed at different ratios of effector-to-target in the absence (B) or presence (C) of 10 nM

FITC-folate adapter. Data are represented as mean  $\pm$  s.d. of five independent replicates, \*p<0.05. ELISA analysis of secreted cytokine IFN $\gamma$  (D) and TNF $\alpha$  (E) from various NK-92 cells upon MDA-MB-231 stimulation was shown. Data are represented as mean  $\pm$  s.d. of five independent replicates, \*p<0.05. (F) Representative flow cytometry analysis of phosphorylated STAT3 (pSTAT3) and STAT5 (pSTAT5) in indicated NK-92 cells upon MDA-MB-231 stimulation. (G) Expansion of indicated NK-92 cells 7 days after co-culture with MDA-MB-231 cells was quantified. Data are represented as mean  $\pm$  s.d. of five independent replicates, \*p<0.05. (H-I) Schematic of *in vitro* MDA-MB-231 tumor rechallenge model and cytotoxicity assay was shown in (H). (I) Killing of MDA-MB-231 tumor cells by indicated NK-92 cells was performed in the presence of 10 nM FITC-folate adapter at different time points. Data are represented as mean  $\pm$  s.d. of five independent replicates, \*p<0.05.

FITC using NK or T cell-specific signaling domains, and CAR #5 to #8 were combinatory dual antigen-targeting CARs. For the switchable anti-FITC scFv CARs, CAR #1, #5, and #7 employ a NK-specific transmembrane domain NKG2D, a co-stimulatory domain 2B4 and an intracellular domain CD3 $\zeta$ , whereas CAR #2, #6, and #8 differ in the transmembrane domain CD8 and co-stimulatory domain 4-1BB. For tumor microenvironment responsive anti-PD-L1 nanobody CARs, CAR #3, #5, and #7 use a NK-specific transmembrane domain NKG2D, a co-stimulatory domain 2B4, a truncated IL-2 receptor  $\beta$ -chain (Delta IL-2RB), an intracellular domain CD3 $\zeta$ , and a STAT3-binding tyrosine-X-X-glutamine (YXXQ) motif, whereas CAR #4, #6, and #8 differ in the transmembrane domain CD28. These CAR constructs were first tested in NK-92 cells for their ability to enhance antitumor activities against FR $\alpha$ + and PD-L1+ tumor cells. Human breast cancer MDA-MB-231 cells express high levels of FR $\alpha$  and PD-L1, whereas human prostate adenocarcinoma LNCaP cells express neither FR $\alpha$  nor PD-L1 (**Fig. S1A**) [44]. These two tumor lines were used for antitumor cytotoxicity analysis of our engineered CAR NK-92 cells.

Bi-specific FITC-folate adapter (FITC-FA) was first synthesized with folic acid on the left reside for binding FR $\alpha$  on breast tumor cells and fluorescein on the right side for anti-FITC CAR targeting (**Fig. S1B**) [39]. The binding affinity ( $K_d$ ) of FITC-folate for MDA-MB-231 tumor cells

was measured as 2.64 nM (**Fig. S1C**), and the affinity ( $K_d$ ) of FITC-folate for various anti-FITC CAR NK-92 cells were about 10 nM (**Fig. S1D**). Considering the fact that insufficient intracellular bridges will be formed at very low FITC-folate concentration, whereas at very high concentrations, intracellular bridging will be locked due to monovalent saturation of ligand binding sites on both cell types with excess FITC-folate adapters, 10 nM of FITC-folate was used in the following studies.

The killing potency of various anti-FITC and/or anti-PD-L1 CAR NK-92 cells (Fig. S1E) were then tested in MDA-MB-231 (FR $\alpha$ + PD-L1+) and LNCaP cell (FR $\alpha$ - PD-L1-) cells. As expected, CAR-expressing NK-92 cells exhibited more potent cytotoxicity against MDA-MB-231 and more cytotoxic granule release than LNCaP cells (Fig. 2B and S2A-D). In the presence of bi-specific FITC-folate adapter, anti-MDA-MB-231 cytotoxicity of CAR NK-92 cells was significantly increased (Fig. 2C), indicating the specificity of our anti-FITC CAR. Among these CARs, CAR #1, #5, and #6 displayed a much larger increase of anti-tumor activity in NK-92 cells against FRα+ PD-L1+ breast cancer cells after bridging with the FITC-folate adapter (Fig. 2C), along with significantly enhanced IFN $\gamma$  and TNF $\alpha$  release (cytotoxic granule) (Fig. 2D-2E). As expected, these FITC-folate bridged NK-CARs (#1, #5, and #6) mediated higher killing potency in NK-92 cells than T cell specific CARs (#2, #7, and #8). To further test the broader applicability of our anti-FITC CAR-NK cells in treating heterogenous solid tumors, we also synthesized a bi-specific FITC-DUPA adapter (Fig. S3A-B) to target prostate specific membrane antigen (PSMA)-expressing prostate tumor cells. As expected, FITC-DUPA-bridged CAR #1, #5, and #6 NK-92 cells lysed more LNCaP cells than MDA-MB-231 cells (Fig. S3C-S3D), confirming the specificity and multi-tumor targeting ability of our anti-FITC CAR.

170

171

172

173

148

149

150

151

152

153

154

155

156

157

158

159

160

161

162

163

164

165

166

167

168

169

## Screening CAR structures with enhanced NK cell proliferation activity

We next evaluated the capability of various CARs in promoting antigen-specific NK cell proliferation after co-culturing with tumor cells. Both truncated IL-2 receptor  $\beta$ -chain ( $\Delta$ IL-2RB

and the STAT3-binding tyrosine-X-X-glutamine (YXXO) motif in the anti-PD-L1 CARs were designed to enhance cell proliferation and persistence via activation of JAK, STAT3 and STAT5 signaling pathways [45]. Upon PD-L1+ MDA-MB-231 cell stimulation, CAR NK-92 cells exhibited upregulated levels of phosphorylated STAT3 (pSTAT3) and pSTAT5 (Fig. 2F), among which CAR #3, #5, and #7 displayed superior ability in upregulating pSTAT3 and pSTAT5 (Fig. **S4A-S4B**). As expected, CAR #3, #5, and #7 also promoted greatest proliferation in NK-92 cells (Fig. 2G). We next constructed a continuous in vitro tumor cell exposure model to investigate the persistence and memory-like phenotype of NK-92 cells after CAR engineering (Fig. 2H). Consistent with previous observation, NK-92 cells engineered with CAR #1, #5 and #6 displayed superior tumor-killing ability against FR $\alpha$ + PD-L1+ breast cancer cells under the initial antigen exposure at day 1 (Fig. 21). As the antigen exposure increases (day 8 and 15), significant reduction of anti-tumor cytotoxicity in NK-92 cells with anti-FITC CAR only (CAR #1), whereas dual anti-FITC and anti-PD-L1 CAR NK-92 cells (CAR #5 and #6) still exhibited excellent antitumor activities at day 15. Notably, dual anti-FITC and anti-PD-L1 CAR #5 with NK-specific transmembrane and co-stimulatory domains presented superior persistence as compared to all other CARs. Recently, memory-like NK cells were induced with a cytokine cocktail of IL-12, IL-15 and IL-18 [15,16]. We next evaluated if cytokine treatment may achieve boosted memory-like phenotype in our dual CAR-NK cells (Fig. S5A). While cytokine treatment increased antitumor cytotoxicity of single anti-PD-L1 CAR NK-92 cells, significant difference was not observed in FITC-FA bridged dual CAR NK-92 cells (Fig. S5B). Our results demonstrated that dual CAR design may synergize multi-functions of NK cells under specific tumor antigen stimulation and achieve a memory-like phenotype with superior antitumor activities and persistence under immunosuppressive tumor microenvironment.

197

198

196

174

175

176

177

178

179

180

181

182

183

184

185

186

187

188

189

190

191

192

193

194

195

### Engineering hPSC-derived NK cells with dual CARs for enhanced function

Given its superior anti-tumor activity and persistence in NK-92 cells, dual anti-FITC and PD-L1 CAR #5 was selected for CAR engineering of hPSC-derived NK cells. Single antigentargeting anti-FITC CAR #1 and anti-PD-L1 CAR #3 was used as a control for anti-tumor cytotoxicity and cell proliferation, respectively. To provide a potentially off-the-shelf source of CAR-expressing NK cells, we engineered hPSCs with these three CARs. We knocked the universal anti-FITC CAR into the AAVSI safe harbor locus via CRISPR/Cas9-mediated homologous recombination [46] (Fig. S6A-B), leading to robust CAR-expressing hPSCs (Fig. **S6C**). Notably, engineered hPSCs retained high level expression of pluripotency markers, including stage-specific embryonic antigen-4 (SSEA-4) and octamer-binding transcription factor 4 (OCT-4) (Fig. S6C). To determine the effect of CAR expression on NK cell differentiation, genetically-modified hPSCs were subjected for hematopoietic [47] and NK cell differentiation [48] using stage-specific morphogens (Fig. S7A). High purity of CD45+CD43+ hematopoietic stem and progenitor cells (HSPCs) (Fig. S7B) and CD56+CD45+ NK cells (Fig. S7C) were successfully generated from wildtype or CAR-expressing hPSCs. The resulting hPSC-derived NK cells also expressed high levels of typical NK cell surface markers, including CD16, KID3DL1, NKp46, NKG2D, and NKp44 (Fig. 3A). To determine their antitumor cytotoxicity, CAR-expressing hPSC-derived NK cells were cocultured with MDA-MB-231 cells in the presence of 10 nM FITC-folate. As compared to wildtype hPSC-NK cells, more immunological synapses were formed between CAR-engineered NK cells within 2 hours (Fig. 3B), and dual CAR-NK cells formed most immunological synapses with tumor cells (Fig. 3C), whereas all hPSC-derived NK cells showed similar and less immunological synapse formation ability against FRα-PD L1- LNCaP prostate cancer cells (Fig. S8A), demonstrating the high specificity of these CARs to the targeted tumor antigens. In response to MDA-MB-231 tumor cells, CAR-NK cells expressed more IFNy and CD107a (Fig. **3D**) and released more cytotoxic granule TNFα and IFNγ (Fig. 3E-3F). As expected, dual CAR-NK cells expressed most IFNy and CD107a, and released the most cytotoxic granule, whereas all

199

200

201

202

203

204

205

206

207

208

209

210

211

212

213

214

215

216

217

218

219

220

221

222

223

tested NK cells expressed low levels of IFN $\gamma$  and CD107a, and released low amount of cytotoxic granule upon FR $\alpha$ -PD-L1- LNCaP cell stimulation (**Fig. S8B-D**). We next assessed the tumor-killing ability of different hPSC-NK cells, and demonstrated that dual CAR-NK cells displayed superior anti-MDA-MB-231 cytotoxicity as compared to wildtype, anti-FITC CAR, and anti-PD-L1 CAR-NK cells (**Fig. 3G**), whereas all hPSC-derived NK cells displayed similar and low cytotoxicity against LNCaP tumor cells (**Fig. S8E**).

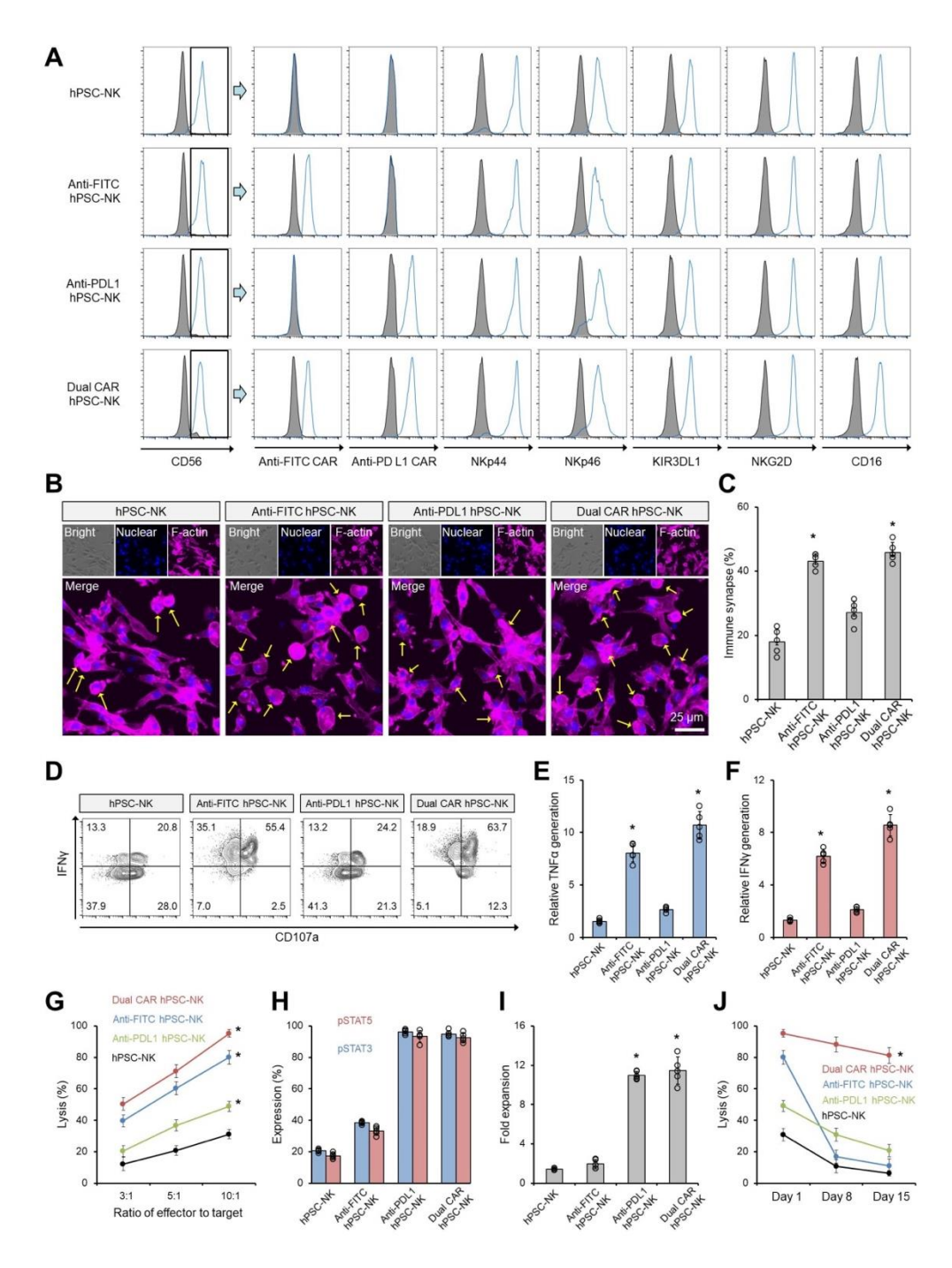
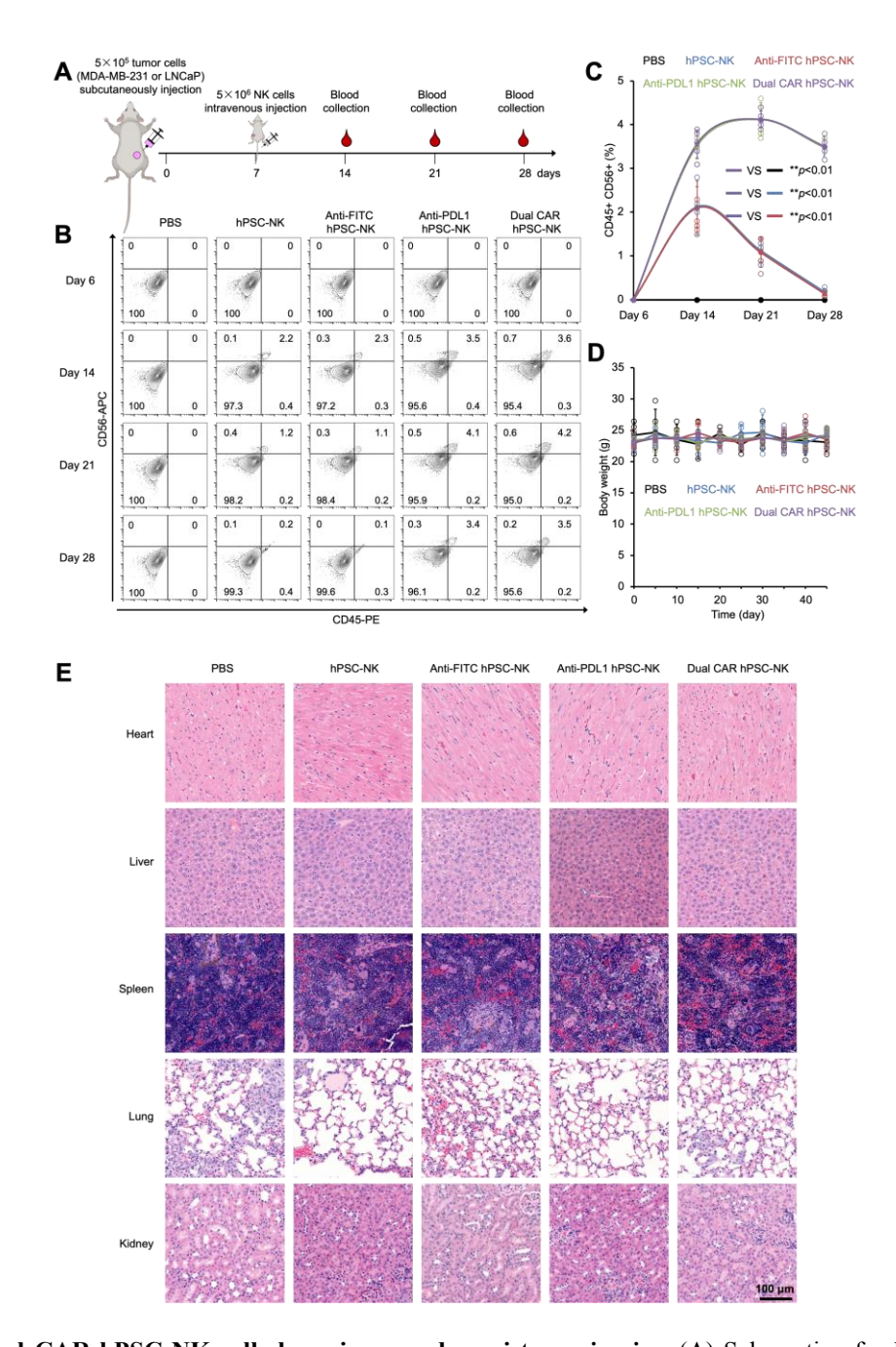


Fig. 3. NK cells derived from chimeric antigen receptor (CAR)-engineered H9 hPSCs display enhanced memory-like antitumor cytotoxicity. (A) Flow cytometry analysis of NK cells derived from different hPSCs. Plots show histograms of control (Black) and indicated NK cell-specific antibody (blue). (B-C) Representative images of immunological synapses at the interface between tumor and indicated hPSC-NK cells by F-actin staining (B) and the numbers of immunological synapses were quantified in (C).

Scale bar, 25  $\mu$ m. (D) Flow cytometry analysis of INF $\gamma$ /CD107a in different NK cells upon MDA-MB-231 cell stimulation. ELISA analysis of secreted cytokine TNF $\alpha$  (E) and INF $\gamma$  (F) from indicated NK cells in response to MDA-MB-231 cells is shown. (G) Killing of MDA-MB-231 tumor cells by indicated hPSC-NK cells was performed at different ratios effector-to-target in the presence of 10 nM FITC-folate adapter. (H) Expression of phosphorylated STAT3 (pSTAT3) and STAT5 (pSTAT5) in the indicated hPSC-NK cells upon MDA-MB-231 stimulation was quantified. (I) Expansion of indicated hPSC-NK cells 7 days after co-culture with MDA-MB-231 tumor cells was quantified. (J) Killing of MDA-MB-231 tumor cells by indicated hPSC-NK cells was performed in the presence of 10 nM FITC-folate adapter at different time points. Data are represented as mean  $\pm$  s.d. of five independent replicates, \*p<0.05.

We then investigated the antigen-responsive proliferation ability of various hPSC-NK cells. Upon PD-L1+ MDA-MB-231 cell stimulation, hPSC-derived CAR-NK cells upregulated expression levels of phosphorylated STAT3 (pSTAT3) and pSTAT5 (Fig. S9A). Single antigentargeting anti-PD-L1 and dual CAR-NK cells exhibited highest expression levels of pSTAT3 and pSTAT5 (Fig. 3H), and achieved highest cell expansion (Fig. 3I). We next investigated the antitumor cytotoxicity and persistence of CAR-NK cells in a continuous antigen exposure model. While similar strong initial anti-MDA-MB-231 cytotoxicity was observed in anti-FITC and dual CAR NK cells at day 1 (Fig. 3J), anti-FITC CAR-NK cells significantly reduced tumor-killing ability as antigen exposure time increase (day 8 and 15), whereas dual CAR-NK cells still exhibited excellent anti-tumor ability and persistence at day 15. Consistent with observation in NK-92 cells, memory-like NK cytokine treatment significantly enhanced antitumor cytotoxicity of hPSC-derived wildtype or single CAR-NK cells (Fig. S9B-C). Significant difference was not observed between FITC-FA bridged dual CAR-NK cells treated with or without cytokine, indicating the memory-like potency of our dual CAR. Importantly, all CAR-expressing hPSCderived NK cells did not kill normal H9 hPSCs and hPSCs-derived somatic cells (Fig. S9D), demonstrating their safety in future clinical applications.



**Fig. 4. Dual CAR-hPSC-NK cells have improved persistence** *in vivo*. (A) Schematic of subcutaneous injection of MDA-MB-231 cells for *in vivo* tumor model construction and persistence analysis of various hPSC-derived NK cells. (B) Flow cytometry analysis of CD45+CD56+ hPSC-NK cells in host blood at different time points after intravenous injection of indicated hPSC-NK cells or PBS control. The percentage of CD45+CD56+ hPSC-NK cells was quantified in (C). n=5. (D) Body weight of all experimental mouse groups was measured at indicated time points. (E) H&E images of major organs collected at the end of treatment are shown.

273

274

275

276

277

278

279

280

281

282

283

284

285

286

287

288

289

290

291

292

293

294

295

### Dual CAR-hPSC-NK cells have improved antigen-responsive persistence in vivo

Systemic administration or ectopic expression of interleukin-15 (IL-15) has been used to improve in vivo persistence of CAR-NK cells [17–19], which though may lead to abnormal cell proliferation, severe adverse events or even leukemia transformation in patients [26]. To determine the effect of anti-PD-L1 CAR on the proliferation and persistence of hPSC-NK cells, NRG mice engrafted with  $5 \times 10^5$  PD-L1-expressing MDA-MB-231 breast cancer cells or PD-L1rare LNCaP cells (Fig. 4A, Fig. S11) were treated with intravenous infusion of  $5 \times 10^6$  different hPSC-derived NK cells or PBS 7 days after tumor cell injection. These CAR NK cells exhibited excellent tumor targeting ability (Fig. S10). Host blood was collected at day 6, 14, 21, and 28 for NK cell analysis, and significantly higher NK cell numbers were detected in the anti-PD-L1 and dual CAR NK groups in the MDA-MB-231 mouse xenograft tumor model than other groups (Fig. **4B-4C**). As expected, low NK cells were detected in all experimental groups of LNCaP xenograft model (Fig. S11A-B), highlighting the specificity of anti-PD-L1 CAR and its capacity to enhance persistence of NK cells in vivo. The biocompatibility of hPSC-derived CAR-NK cells was also evaluated by monitoring the body weight of host mice, and there was no significant body weight loss across all tested experimental groups (Fig. 4D, S10C), indicating the minimal systemic toxicity and high biocompatibility of hPSC-derived NK cells. Histological analysis of major organs sliced from host mice at day 30 showed that adoptive NK cells did not cause any observable abnormality or damage in heart, liver, spleen, lung, and kidney (Fig. 4E), which was further supported by the blood biochemistry analysis (Table S2), confirming the biocompatibility of our hPSC-derived NK cells.

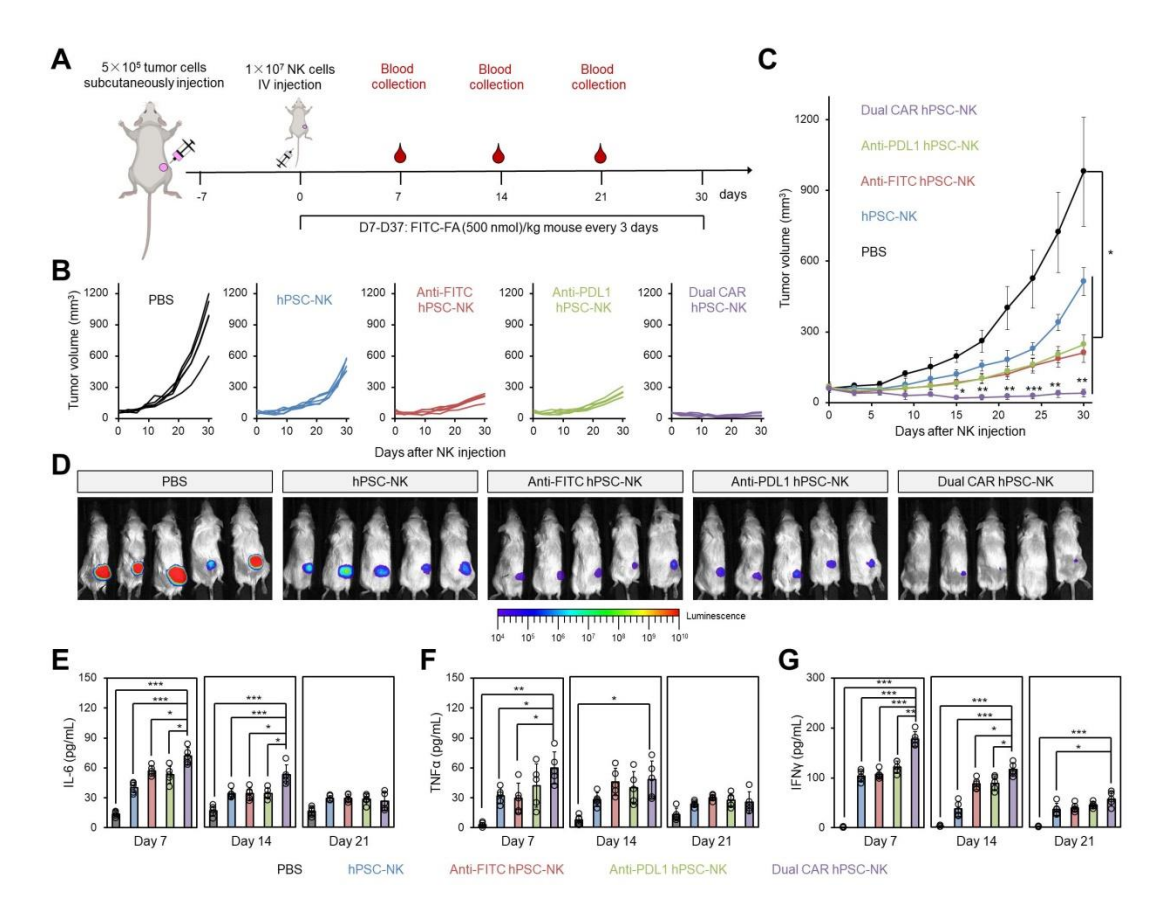


Fig. 5. In vivo anti-tumor activities of various hPSC-NK cells were assessed via intravenous injection.

(A) Schematic of intravenous injection of various hPSC-NK cells for *in vivo* anti-tumor cytotoxicity study.  $5\times10^5$  MDA-MB-231 cells were subcutaneously implanted into the right back of NRG mice. After 7 days, mice were intravenously treated with PBS or  $1\times10^7$  hPSC-NK cells. (B-C) Time-dependent tumor burden was measured and quantified for indicated experimental mouse groups. \*p<0.05, \*\*p<0.01, and \*\*\*p<0.001. (D) Representative photos of tumor-bearing mice at the end of treatment. Levels of released human tumor necrosis factor- $\alpha$  (TNF $\alpha$ ) (E), IL-6 (F), and interferon gamma (IFN $\gamma$ ) (G) in peripheral blood collected from indicated experimental mice were measured by ELISA. n=5. \*p<0.05, \*\*p<0.01, and \*\*\*p<0.001.

## Dual CAR-hPSC-NK cells have improved antitumor activities in tumor rechallenge models

To evaluate antitumor activities of different hPSC-NK cells *in vivo*, we first tested cytotoxicity of MDA-MB-231 cells in a mouse xenograft model. Mice were subcutaneously injected with 5×

10<sup>5</sup> MDA-MB-231 cells and systemically administered a single injection of  $1 \times 10^7$  NK cells 7 days after tumor inoculation (**Fig. 5A**). As compared to the tumor-bearing mice treated with PBS, administration of hPSC-NK cells significantly reduced tumor burden (**Fig. 5B-D**). As expected, dual CAR hPSC-NK cells displayed higher anti-tumor cytotoxicity than wildtype or other CAR-expressing NK cells. We next measured human cytokine production release in the plasma of different experimental mouse groups, including TNFα, IL-6 and IFNγ. All non-PBS experimental groups released detectable TNFα and IL-6 in the plasma from day 14 to day 28, and dual CAR hPSC-NK cells maintained highest levels of both cytokines (**Fig. 5E-F**), which were eventually decreased in host mice, indicating a reduced risk of cytokine release syndrome. The superior production of IFNγ in dual CAR-NK cells (**Fig. 5G**) is also consistent with their memory-like phenotype [15,16].

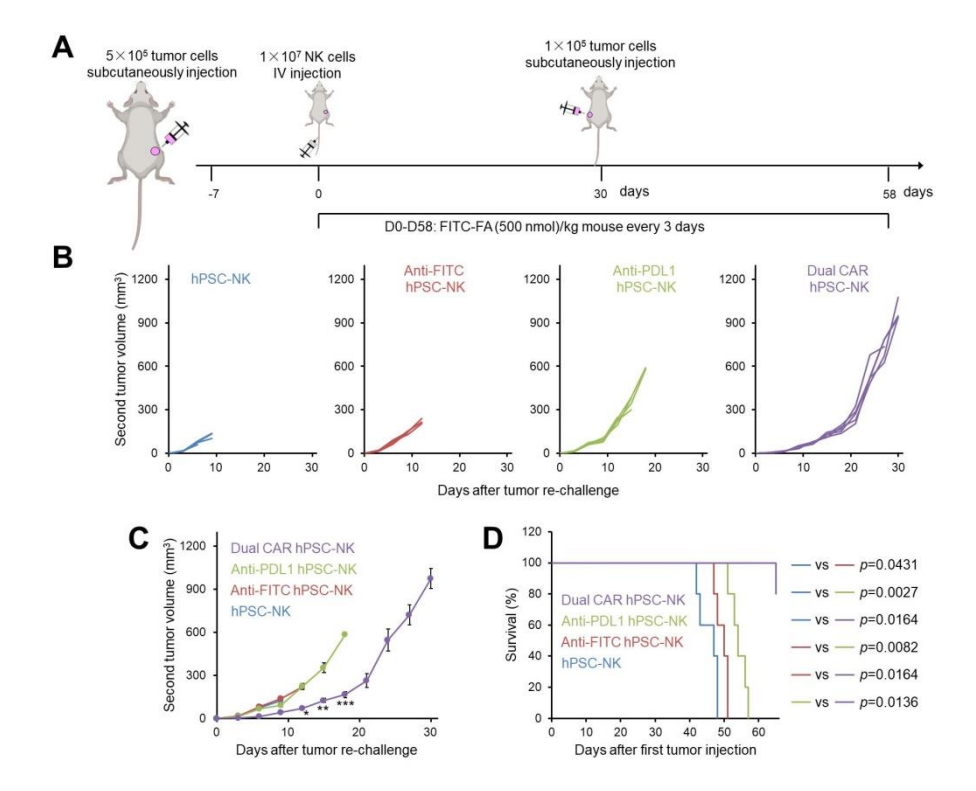


Fig. 6. Dual CAR-hPSC-NK cells have improved antitumor activities in an *in vivo* tumor rechallenge model. (A) Schematic of the *in vivo* tumor rechallenge model, in which 1×10<sup>5</sup> MDA-MB-231 cells were subcutaneously implanted into the left back of NSG mice at day 37. (B-C) Time-dependent second tumor

burden was measured and quantified for indicated experimental mouse groups. Experimental mice were sacrificed when the primary tumor size reaches 1000 mm<sup>3</sup>. (D) Kaplan-Meier Curve demonstrating survival of indicated experimental mouse groups was shown. n=5.

Given the promising *in vivo* performance of our hPSC-derived NK cells, MDA-MB-231 tumor cells were re-inoculated to construct a tumor rechallenge model for the investigation of their memory-like behavior (**Fig. 6A**). Compared with other experimental groups, dual CAR hPSC-NK cells significantly slowed down the growth of second tumor (**Fig. 6B-6C** and **Fig. S12**) and prolonged the survival of tumor-bearing mice (**Fig. 6D**). Our data indicate that the combination of tumor microenvironment responsive anti-PD-L1 and programmable anti-FITC CARs significantly enhances *in vivo* persistence and antitumor activities of hPSC-derived NK cells, endowing them with a memory-like capacity for improved immunotherapy.

#### **DISCUSSION**

Due to their innate immunity against all kinds of pathogen and unique property of not causing GvHD in allogenic transplantation, adoptive CAR-NK cell therapy holds great promise in treating various cancers. To date, most efforts have been conducted to treat hematologic malignancies with FDA-approved anti-CD19 or anti-CD33 CAR NK cells [18,49–51]. CARs targeting various solid tumors, such as EGFR<sup>+</sup> breast cancer [52,53], EGFR<sup>+</sup>/HER2<sup>+</sup> glioblastoma [17,54], and PSMA<sup>+</sup> prostate cancer [55], are also developed for preclinical and clinical studies. While none of the 11 patients in a phase I/II trial developed severe toxicity [51], concerns still exist regarding the off-tumor effects, sustained effector cell proliferation and exhaustion, cytokine release syndrome (CRS), and CAR specificity against targeted tumor, particularly in antigenheterogeneous cancers. To circumvent these concerns in CAR-T cells [56], we have previously developed a universal anti-FITC CAR strategy, in which cancer cell killing can be precisely controlled by regulating doses of a bispecific adapter and CAR expression on T cells can be

sensitively regulated by a fluorescein-linked TLR7, to selectively activate CAR-T cells and sensitively manage a CRS [36,39]. Such concerns may also be observed in adoptive CAR-NK cell therapies, posing a significant barrier for their clinical translation. To develop a safer CAR-NK cell therapy that are truly universal and potent, we equipped NK cells with a stable anti-FITC CAR, and demonstrated the controllable and potent antitumor activities of hPSC-derived CAR-NK and CAR-NK-92 cells, though a comprehensive safety profile of our CAR-NK cells is still needed in future preclinical and clinical studies. In the pursuit of achieving higher efficacy and potency in NK cells, we also added a second anti-PD-L1 CAR in our CAR-NK cells due to the striking clinical efficacy shown by checkpoint inhibitors that target PD-1 or PD-L1. Targeting PD-L1 may allow selective targeting of solid tumor cells and side effect profiles would be predicted based on PD-1/L1 immune checkpoint blockade [57]. Clinical trials with anti-PD-L1 CAR-NK cells are also currently underway (NCT04847466). Unlike previous CD28 transmembrane and FceRIy signaling domains [57,58], our CAR construct contains a NK-specific NKG2D transmembrane domain, and a CD3\(\zeta\) signaling domain that is essential for both T and NK cell activation [59]. We also incorporated a NK-specific 2B4 co-stimulatory domain [33] into our CAR construct, and instead of scFv, we used a smaller anti-PD-L1 nanobody for tumor antigen targeting [60]. CAR-NK cells bearing an anti-FITC CAR showed significantly improved antitumor activity, both in vitro and in vivo, after engineering with the anti-PD-L1 CAR. While we have demonstrated the therapeutic potential of our dual CAR-NK cells in the immunodeficient mice, other preclinical models with an intact immune system, such as humanized mouse models with human immune T cells, and orthotopic tumor implantation are needed to better assess the safety and efficacy of hPSC-derived CAR-NK cells. Primary mature NK cells present a short-lived phenotype in vivo [61], imparting a poor persistence in xenograft tumor models and human cancer patients [18]. Recent studies have demonstrated that mouse and human NK cells display memory-like in response to viral infection

351

352

353

354

355

356

357

358

359

360

361

362

363

364

365

366

367

368

369

370

371

372

373

374

375

[14,62–64], certain hapten exposure [64], and/or a brief treatment with cytokines of IL-12, IL-15 and IL-18 [10,16,20-22], leading to the increased longevity and improved effector function of NK cells in preclinical and clinical models. However, more enhanced NK cell persistence in vivo is still urgently needed to achieve sustained clinical benefits in various cancers, particularly in solid tumors. Systemic administration or ectopic expression of IL-15 has been widely used to improve in vivo persistence of various NK cells [17–19], which may lead to autonomous NK cell proliferation, severe adverse effects, or even leukemia transformation in patients [26]. IL-15 was also linked to a lymphoma/leukemia-targeting CD19 CAR via a 2A sequence peptide to improve in vivo persistence and antitumor functions of cord blood NK cells [18,65]. IL-15 activates STAT5 signaling via IL-2 receptor β-chain (IL-2Rβ), and thus we directly added a truncated IL-2Rβ (ΔIL-2Rβ) domain [45] into our tumor microenvironment responsive anti-PD-L1 CARs to achieve antigen-inducible NK cell expansion. Since IL-21 plays a critical role in memory cell formation [66], reverses NK cell exhaustion [34], and promotes expansion of memory-like NK cells [67,68], we also incorporated into our anti-PD-L1 CAR construct a STAT3 signaling activation motif YXXQ, an IL-21-associated residue within the IL-21 receptor. Such modifications have led to robust activation of STAT3 and STAT5 signaling pathway in a tumor antigen-responsive manner, and to CAR-NK cells with enhanced in vivo persistence and antitumor functions than that seen with single anti-FITC CAR NK cells lacking an anti-PD-L1 CAR. Cell expansion was not observed in CAR-NK cells with the anti-PD-L1 CAR co-culturing with PD-L1 rare tumor cells, further demonstrating the antigen specificity of our CAR-NK cell persistence for a safer and more durable antitumor immunity. CAR-NK cells have been engineered from various NK cells, including NK-92 cell line, hPSCderived, cord blood and peripheral blood NK cells, though NK-92 derived CAR-NK cells are dominant in clinical trials due to its excellent expansion capacity in vitro. While no obvious toxicity was observed in clinical trials with NK-92 cells [69], concerns still exist regarding their in vivo survival and proliferation after irradiation during cell preparation for infusion [33].

377

378

379

380

381

382

383

384

385

386

387

388

389

390

391

392

393

394

395

396

397

398

399

400

401

Alternatively, engineering CAR-NK cells from hPSCs has allowed an unlimited cell source of truly off-the-shelf cellular products for clinical trials [33]. In addition, the relative ease of genome editing in hPSCs also allows massive production of homogenous and stable CAR-expressing NK cells for a more standardized product on a clinical scale. In this study, we demonstrated that both CRISPR/Cas9-mediated knockin and lentiviral transduction strategies could be used to introduce CAR constructs into hPSCs for functional CAR-NK cell production.

In conclusion, we have developed a novel immunoengineering approach in which hPSCs are engineered with dual CAR constructs and differentiated into off-the-shelf CAR-NK cellular products. The dual anti-FITC and anti-PD-L1 hPSC CAR-NK cells are designed and demonstrated with improved universality, safety, potency, and persistence, both *in vitro* and *in vivo*, in an antigen-dependent manner, achieving a memory-like phenotype of NK cells.

### EXPERIMENTAL SECTION

CAR plasmid construction. To construct anti-PD-L1 lentiviral vectors, DNA sequence encoding CD8a signal peptide, anti-PD-L1 nanobody [60], CD28 extracellular domain, CD28 or NKG2D transmembrane domain, CD28 or 2B4 intracellular co-stimulatory domain, ΔIL-2Rβ, CD3ζ-YXXQ was directly synthesized and cloned into the lenti-luciferase-P2A-NeoR (Addgene #105621) backbone via NEBuilder HiFi DNA Assembly after BamHI and MluI digestion. The resulting anti-PD-L1 plasmids were then sequenced and digested with MluI to further incorporate an IRES-NeoR or IRES-GFP sequence. The anti-FITC CAR plasmid with CD8a signal peptide, anti-fluorescein scFv, CD8a extracellular and intracellular domains, 4-1BB co-stimulatory domain and CD3ζ signaling domain was previously constructed in our lab [39] and cloned into our AAVS1-Puro CAG FUCCI donor plasmid [46] (Addgene #136934). The resulting AAVS1-Puro CAG anti-FITC-CAR plasmid was digested with SgrDI and MluI, and ligated to the lentiviral anti-PD-L1 CAR backbone to construct the lentiviral anti-FITC CAR vector. To make anti-FITC CAR plasmid with NKG2D transmembrane and 2B4 co-stimulatory domains, anti-

FITC scFv sequence and chimeric sequence of NKG2D, 2B4 and CD3ζ were PCR amplified from lentiviral anti-FITC CAR vector and AAVS1-Puro CAG CLTX-NKG2D-2B4-CD3z CAR (Addgene #157744), respectively, and cloned into AAVS1-Puro CAG FUCCI plasmid via NEBuilder HiFi DNA Assembly to make AAVS1-Puro CAG anti-FITC-NKG2D-2B4-CD3z CAR, which was digested with SgrDI and MluI, and ligated to the lentiviral anti-PD-L1 CAR backbone to construct the lentiviral anti-FITC-NKG2D-2B4-CD3z CAR.

435

436

437

438

439

440

441

442

443

444

445

446

447

448

449

450

451

429

430

431

432

433

434

Maintenance and differentiation of hPSCs. H9 hPSC line was obtained from WiCell and maintained on Matrigel-coated plates in mTeSR plus medium. For NK cell differentiation, hPSCs were dissociated with 0.5 mM EDTA and seeded onto iMatrix 511-coated 24-well plate at a cell density between 10, 000 and 80, 000 cells/cm<sup>2</sup> in mTesR plus medium with 5 µM Y27632 for 24 hours (day -1). At day 0, cells were treated with 6 μM CHIR99021 (CHIR) in DMEM medium supplemented with 100 µg/mL ascorbic acid (DMEM/Vc), followed by a medium change with LaSR basal medium from day 1 to day 4. 50 ng/mL VEGF was added to the medium from day 2 to day 4. At day 4, medium was replaced by Stemline II medium (Sigma) supplemented with 10 μM SB431542, 25 ng/mL SCF and FLT3L. On day 6, SB431542-containing medium was aspirated and cells were maintained in Stemline II medium with 50 ng/mL SCF and FLT3L. At day 9 and day 12, top half medium was aspirated and replaced with 0.5 mL of fresh Stemline II medium containing 50 ng/mL SCF and FLT3L. At day 15, floating cells were gently harvested, filtered with a cell strainer, and co-culture on OP9-DLL4 (kindly provided by Dr. Igor Slukvin) monolayer (2 ×10<sup>4</sup> cells/mL) in NK cell differentiation medium: α-MEM medium supplemented with 20% fetal bovine serum (FBS), 5 ng/mL IL-7, 5 ng/mL FTL3L, 25 ng/mL SCF, 5 ng/mL IL-15, and 35 nM UM171. NK cell differentiation medium was changed every 3 days, and floating cells were transferred onto fresh OP9-DLL4 monolayer every 6 days.

453

Lentivirus production and hPSC transduction. For lentivirus production, 293TN cells were incubated in DMEM medium containing 10% fetal bovine serum (FBS), 1% sodium pyruvate, and 0.5% GlutaMAX until 95-100% confluence. 4.5 µg lentiviral CAR plasmid, 3.0 µg psPAX2, and 1.5 µg pMD2.G were added to 450 µL of Opti-MEM medium and incubated at room temperature for 5 minutes. 27 µL of FuGENE HD reagent was then added to the mixture and incubated at room temperature for another 15 minutes. The resulting 450 µL plasmid mixture was added to 3 mL of culture medium and evenly distributed to 3 wells of 6 well plate with 293TN cells after aspirating the old medium. 18 hours after plasmid addition, aspirate the medium from each well and replace with 3 mL of fresh culture medium, and incubated for another 24 hours. Virus-containing supernatant was then collected every day with fresh warm medium change for 2 to 3 days, transferred to a 50 mL conical tube, and stored at 4 °C. The resulting virus supernatant were then centrifuged at 2, 000 g at 4 °C for 5 minutes or filtered through a 0.45 µm filter to remove cell debris. For hPSC transduction, hPSCs were dissociated with 0.5 mM EDTA and seeded onto iMatrix 511-coated 6-well plate at a cell density between 10, 000 and 80, 000 cells/cm<sup>2</sup> in mTesR plus medium with 5 μM Y27632. 24 hour later, stem cell culture medium was aspirated and replaced with 1 mL of mTesR plus medium with 5 μM Y27632 and 1 mL of virus supernatant, which were removed and replaced with 2 mL of fresh mTeSR plus after 24 hour. 2 to 3 days after transduction, 300 µg/ml G418 or 1 µg/mL puromycin was applied to select successfully transduced hPSCs. To further enrich desired cells, transduced hPSCs were dissociated and transferred to 96-well plate at a cell density of 10 cells/mL. After a 4-day culture, hPSCs were continuously treated with 300 µg/ml G418 or 1 µg/mL puromycin for 8 more days.

475

476

477

478

479

454

455

456

457

458

459

460

461

462

463

464

465

466

467

468

469

470

471

472

473

474

**NK-92 cell maintenance and lentiviral transduction.** NK-92 cells were cultured in MyeloCult H5100 medium containing 100 units/mL human recombinant IL-2. For lentiviral transduction, NK-92 cells were stimulated by IL-2 and IL-15 firstly. Briefly, count the NK-92 cells and resuspend them in appropriate medium (RPMI 1640, 10% FBS, 2 nM L-glutamine, 20 ng/mL IL-

2, 50 ng/mL IL-15, and 100 ng/mL IL-12) at 1×10<sup>6</sup> cells/mL. These NK-92 cells were stimulated for 2 hours before lentiviral transduction. After cytokine stimulation, 1×10<sup>5</sup> NK-92 cells were plated in each well of a 12-well plate, and cells were treated with 1 mL virus supernatant and polybrene (8 μg/mL) overnight at 37 °C, 5% CO<sub>2</sub>. After 24 hours, viruses were removed by centrifuging at 360 xg for 5 minutes, and the resulting NK-92 cells were suspended in 1 mL MyeloCult H5100 medium with 100 units/mL human recombinant IL-2. After 5 days, transduced NK-92 cells were centrifuged at 360 xg for 5 minutes and resuspended in 1 mL MyeloCult H5100 medium containing 100 units/mL human recombinant IL-2 and 1 μg/mL puromycin or 300 μg/ml G418. At least 8-day drug screening is needed to enrich successfully transduced NK-92 cells.

MDA-MB-231 and LNCaP cell maintenance. LNCaP tumor cells were kindly provided and cultured by the laboratory of Dr. Chang-Deng Hu at Purdue University. MDA-MB-231 cells were cultured in Leibovitz's L-15 medium (containing 10% FBS, 100 units mL-1 penicillin and 100 mg mL-1 streptomycin), and LNCaP cells were cultured in RPMI-1640 medium (containing 10% FBS, 100 units mL-1 penicillin and 100 mg mL-1 streptomycin). These two cell lines were incubated at 37 °C, 5% CO<sub>2</sub>. The culture medium was changed every two days and cells passaged at 70-80% confluency.

Flow cytometry analysis. Differentiated cells were gently pipetted and filtered through a 70 or 100 μm strainer. The cells were then pelleted by centrifugation and washed twice with PBS -/-solution containing 1% bovine serum albumin (BSA). Cells were stained with appropriate conjugated or non-conjugated antibodies (**Table S1**) for 30 minutes at room temperature in dark and analyzed in an Accuri C6 plus cytometry (Beckton Dickinson) after washing with BSA-containing PBS -/- solution. FlowJo software was used to analyze the collected data.

NK cell-mediated *in vitro* cytotoxicity assay. The cell viability was analyzed by flow cytometry according to a previous protocol [70]. Briefly, tumor cells were stained with 2 μM Calcein-AM in MEM medium at 37 °C for 10 min in dark, followed by 10% FBS treatment for 10 min in dark at room temperature. Labeled tumor cells were pelleted at 300 x g for 7 min and resuspended in culture medium with 10% FBS at a density of 50,000 cells/mL. 100 μL of tumor cells were then mixed with 100 μL of 150,000, 250,000, and 500,000 cells/mL NK cells in 96 well plates with or without FITC-folate (10 nmol/L), and incubated at 37 °C, 5% CO<sub>2</sub> for 12 hours. To harvest all the cells, cell-containing medium was firstly transferred into a new round-bottom 96-well plate, and 50 μL trypsin-EDTA was added to the empty wells to dissociate attached cells. After 5 min incubation at 37 °C, dissociated cells were transferred into the same wells of round-bottom 96-well plate with floating cells. All cells were pelleted by centrifuging (300 x g, 4 °C, 5 min), and washed with 200 μL of PBS-/- solution containing 0.5% BSA. The pelleted cells were stained with propidium iodide (PI) for 15 min at room temperature, and analyzed in the Accuri C6 plus cytometer (Beckton Dickinson).

Conjugate formation assay. To visualize immunological synapses, 100  $\mu$ L of tumor cells (50,000 cells/mL) were seeded onto wells of 96-well plate and incubated at 37 °C for 12 hours, allowing them to attach. 100  $\mu$ L NK cells (500,000 cells/mL) were then added onto the target tumor cells and incubated for 6 hours before fixing with 4% paraformaldehyde (in PBS). Cytoskeleton staining was then performed using an F-actin Visualization Biochem Kit (Cytoskeleton Inc.).

**ELISA analysis**. To analyze the cytokine production by ELISA assay, 100  $\mu$ L of tumor cells (50,000 cells/mL) were seeded onto wells of 96-well plate and incubated at 37 °C for 12 hours, allowing them to attach. 100  $\mu$ L NK cells (500,000 cells/mL) with or without FITC-folate (10 nmol/L) were then added onto the target tumor cells and incubated for 6 hours. Afterwards, plates

were centrifuged at 350 xg for 10 minutes to spin down the cell debris, and 10  $\mu$ L top supernatant was collected for measuring the TNF $\alpha$  and IL-6 production using an ELISA kit (ThermoFisher Scientific, US).

534

535

536

537

538

539

540

541

542

543

544

545

531

532

533

MDA-MG-231 xenograft studies. All the mouse experiments were approved by the Purdue Use Committee (PACUC). The immunodeficient Animal Care and NOD.Cg-RAG<sup>1tm1Mom</sup>IL2rg<sup>tm1Wjl</sup>/SzJ (NRG) mice were bred and maintained by the Biological Evaluation Core at the Purdue University Center for Cancer Research. MDA-MB-231 cells (5×10<sup>5</sup> tumor cells/per mouse) were implanted subcutaneously. When the tumor size reached ~100 mm<sup>3</sup>, NK cells and FITC-folate were intravenously injected. Mice were maintained on folic acid-deficient diet (TD.95247, Envigo) in order to reduce the level of folic acid in mice to a physiological level found in humans. Tumors were measured the other day with caliper, and tumor volume was calculated according to the equation: tumor volume =  $L \times W^2 \times 1/2$ , where L is the longest axis of the tumor and W is the axis perpendicular to L. Mouse blood was also collected for NK cell and cytokine release (TNFα and IL-6) analysis, and systemic toxicity was monitored by measuring body weight loss of experimental mice.

547

548

549

550

551

546

**Statistical analysis**. Data are presented as mean  $\pm$  standard deviation (SD). Statistical significance was determined by Student's *t*-test (two-tail) between two groups, and three or more groups were analyzed by one-way analysis of variance (ANOVA). P<0.05 was considered statistically significant.

552

553

554

555

#### **ACKNOWLEDGEMENTS**

We thank members of the Low and Bao laboratories for technical assistance. We're also gratefully acknowledge the Purdue Flow Cytometry and Cell Separation Facility, Purdue

Genomics Core Facility and the Biological Evaluation Core at Purdue University Center for 556 557 Cancer Research (PCCR). This study was supported by startup funding from the Davidson School 558 of Chemical Engineering and the College of Engineering at Purdue (X.B.), PCCR Robbers New 559 Investigators (X.B.), Showalter Research Trust (Young Investigator Award to X.B.), NSF CBET 560 (grant no. 2143064 to X.B.), NSF CBET (grant no. 1943696 to X.L.L.), and NIH NCI (grant no. R37CA265926 to X.B.). The authors also gratefully acknowledge support from the Purdue 561 562 University Center for Cancer Research, P30CA023168, Purdue Institute for Integrative Neuroscience (PIIN) and Bindley Biosciences Center, and the Walther Cancer Foundation. 563

564

565

#### CONFLICT OF INTERESTS

A patent related to this manuscript is under application (Y.C., J.J., P.S.L., and X.B.).

567

568

#### REFERENCE

- M.W. Rohaan, S. Wilgenhof, J.B.A.G. Haanen, Adoptive cellular therapies: the current landscape,
   Virchows Arch. (2019). https://doi.org/10.1007/s00428-018-2484-0.
- 571 [2] C.S. Hinrichs, S.A. Rosenberg, Exploiting the curative potential of adoptive T-cell therapy for cancer, Immunol. Rev. (2014). https://doi.org/10.1111/imr.12132.
- 573 [3] A. Redeker, R. Arens, Improving adoptive T cell therapy: The particular role of T cell costimulation, cytokines, and post-transfer vaccination, Front. Immunol. (2016).
- 575 https://doi.org/10.3389/fimmu.2016.00345.
- 576 [4] H. Zhu, R.H. Blum, D. Bernareggi, E.H. Ask, Z. Wu, H.J. Hoel, Z. Meng, C. Wu, K.L. Guan, K.J.
- 577 Malmberg, D.S. Kaufman, Metabolic Reprograming via Deletion of CISH in Human iPSC-Derived
- NK Cells Promotes In Vivo Persistence and Enhances Anti-tumor Activity, Cell Stem Cell. (2020).
- 579 https://doi.org/10.1016/j.stem.2020.05.008.
- 580 [5] B.H. Goldenson, H. Zhu, Y.Z.M. Wang, N. Heragu, D. Bernareggi, A. Ruiz-Cisneros, A. Bahena,
- 581 E.H. Ask, H.J. Hoel, K.J. Malmberg, D.S. Kaufman, Umbilical Cord Blood and iPSC-Derived
- Natural Killer Cells Demonstrate Key Differences in Cytotoxic Activity and KIR Profiles, Front.
- 583 Immunol. (2020). https://doi.org/10.3389/fimmu.2020.561553.
- 584 [6] F. Cichocki, R. Bjordahl, S. Gaidarova, S. Mahmood, R. Abujarour, H. Wang, K. Tuininga, M.
- Felices, Z.B. Davis, L. Bendzick, R. Clarke, L. Stokely, P. Rogers, M. Ge, M. Robinson, B. Rezner,
- D.L. Robbins, T.T. Lee, D.S. Kaufman, B.R. Blazar, B. Valamehr, J.S. Miller, iPSC-derived NK

- cells maintain high cytotoxicity and enhance in vivo tumor control in concert with T cells and anti-
- PD-1 therapy, Sci. Transl. Med. (2020). https://doi.org/10.1126/scitranslmed.aaz5618.
- 589 [7] H. Zhu, R.H. Blum, R. Bjordahl, S. Gaidarova, P. Rogers, T.T. Lee, R. Abujarour, G.B. Bonello, J.
- Wu, P.F. Tsai, J.S. Miller, B. Walcheck, B. Valamehr, D.S. Kaufman, Pluripotent stem cell-derived
- 591 NK cells with high-affinity noncleavable CD16a mediate improved antitumor activity, Blood.
- 592 (2020). https://doi.org/10.1182/blood.2019000621.
- 593 [8] Y. Chang, X. Bao, Adoptive natural killer cell therapy: a human pluripotent stem cell perspective,
- 594 Curr. Opin. Chem. Eng. (2020). https://doi.org/10.1016/j.coche.2020.08.008.
- 595 [9] R. Handgretinger, P. Lang, M.C. André, Exploitation of natural killer cells for the treatment of
- acute leukemia, Blood. (2016). https://doi.org/10.1182/blood-2015-12-629055.
- 597 [10] R. Romee, M. Rosario, M.M. Berrien-Elliott, J.A. Wagner, B.A. Jewell, T. Schappe, J.W. Leong, S.
- Abdel-Latif, S.E. Schneider, S. Willey, C.C. Neal, L. Yu, S.T. Oh, Y.S. Lee, A. Mulder, F. Claas,
- 599 M.A. Cooper, T.A. Fehniger, Cytokine-induced memory-like natural killer cells exhibit enhanced
- responses against myeloid leukemia, Sci. Transl. Med. (2016).
- https://doi.org/10.1126/scitranslmed.aaf2341.
- 602 [11] A. Cerwenka, L.L. Lanier, Natural killer cell memory in infection, inflammation and cancer, Nat.
- Rev. Immunol. (2016). https://doi.org/10.1038/nri.2015.9.
- 604 [12] S. Paust, U.H. Von Andrian, Natural killer cell memory, Nat. Immunol. (2011).
- https://doi.org/10.1038/ni.2032.
- 606 [13] T.E. O'Sullivan, J.C. Sun, L.L. Lanier, Natural Killer Cell Memory, Immunity. (2015).
- https://doi.org/10.1016/j.immuni.2015.09.013.
- 508 [14] J.C. Sun, J.N. Beilke, L.L. Lanier, Adaptive immune features of natural killer cells, Nature. (2009).
- https://doi.org/10.1038/nature07665.
- 610 [15] M.M. Berrien-Elliott, J.A. Wagner, T.A. Fehniger, Human Cytokine-Induced Memory-Like
- 611 Natural Killer Cells, J. Innate Immun. (2015). https://doi.org/10.1159/000382019.
- 612 [16] M.A. Cooper, J.M. Elliott, P.A. Keyel, L. Yang, J.A. Carrero, W.M. Yokoyama, Cytokine-induced
- 613 memory-like natural killer cells, Proc. Natl. Acad. Sci. U. S. A. (2009).
- https://doi.org/10.1073/pnas.0813192106.
- 615 [17] R. Ma, T. Lu, Z. Li, K.Y. Teng, A.G. Mansour, M. Yu, L. Tian, B. Xu, S. Ma, J. Zhang, T. Barr, Y.
- Peng, M.A. Caligiuri, J. Yu, An oncolytic virus expressing il15/il15ra combined with off-the-shelf
- egfr-car nk cells targets glioblastoma, Cancer Res. (2021). https://doi.org/10.1158/0008-
- 618 5472.CAN-21-0035.
- 619 [18] E. Liu, Y. Tong, G. Dotti, H. Shaim, B. Savoldo, M. Mukherjee, J. Orange, X. Wan, X. Lu, A.
- 620 Reynolds, M. Gagea, P. Banerjee, R. Cai, M.H. Bdaiwi, R. Basar, M. Muftuoglu, L. Li, D. Marin,
- W. Wierda, M. Keating, R. Champlin, E. Shpall, K. Rezvani, Cord blood NK cells engineered to
- express IL-15 and a CD19-targeted CAR show long-term persistence and potent antitumor activity,
- 623 Leukemia. (2018). https://doi.org/10.1038/leu.2017.226.

- 624 [19] Z. Du, Y.Y. Ng, S. Zha, S. Wang, piggyBac system to co-express NKG2D CAR and IL-15 to
- augment the in vivo persistence and anti-AML activity of human peripheral blood NK cells, Mol.
- Ther. Methods Clin. Dev. (2021). https://doi.org/10.1016/j.omtm.2021.10.014.
- 627 [20] R. Romee, S.E. Schneider, J.W. Leong, J.M. Chase, C.R. Keppel, R.P. Sullivan, M.A. Cooper, T.A.
- Fehniger, Cytokine activation induces human memory-like NK cells, Blood. (2012).
- https://doi.org/10.1182/blood-2012-04-419283.
- 630 [21] M. Gang, N.D. Marin, P. Wong, C.C. Neal, L. Marsala, M. Foster, T. Schappe, W. Meng, J. Tran,
- M. Schaettler, M. Davila, F. Gao, A.F. Cashen, N.L. Bartlett, N. Mehta-Shah, B.S. Kahl, M.Y. Kim,
- 632 M.L. Cooper, J.F. DiPersio, M.M. Berrien-Elliott, T.A. Fehniger, CAR-modified memory-like NK
- cells exhibit potent responses to NK-resistant lymphomas, Blood. (2020).
- https://doi.org/10.1182/BLOOD.2020006619.
- 635 [22] S. Lopez-Vergès, J.M. Milush, S. Pandey, V.A. York, J. Arakawa-Hoyt, H. Pircher, P.J. Norris,
- D.F. Nixon, L.L. Lanier, CD57 defines a functionally distinct population of mature NK cells in the
- 637 human CD56dimCD16+ NK-cell subset, Blood. (2010). https://doi.org/10.1182/blood-2010-04-
- 638 282301.
- 639 [23] K. Skak, K.S. Frederiksen, D. Lundsgaard, Interleukin-21 activates human natural killer cells and
- modulates their surface receptor expression, Immunology. (2008). https://doi.org/10.1111/j.1365-
- 641 2567.2007.02730.x.
- 642 [24] A. Heinze, B. Grebe, M. Bremm, S. Huenecke, T.A. Munir, L. Graafen, J.T. Frueh, M. Merker, E.
- Rettinger, J. Soerensen, T. Klingebiel, P. Bader, E. Ullrich, C. Cappel, The Synergistic Use of IL-
- 15 and IL-21 for the Generation of NK Cells From CD3/CD19-Depleted Grafts Improves Their ex
- vivo Expansion and Cytotoxic Potential Against Neuroblastoma: Perspective for Optimized
- Immunotherapy Post Haploidentical Stem Cell Trans, Front. Immunol. (2019).
- https://doi.org/10.3389/fimmu.2019.02816.
- 648 [25] M. Ma, S. Badeti, J.K. Kim, D. Liu, Natural Killer (NK) and CAR-NK Cell Expansion Method
- using Membrane Bound-IL-21-Modified B Cell Line, J. Vis. Exp. (2022).
- https://doi.org/10.3791/62336.
- 651 [26] A. Mishra, S. Liu, G.H. Sams, D.P. Curphey, R. Santhanam, L.J. Rush, D. Schaefer, L.G.
- Falkenberg, L. Sullivan, L. Jaroncyk, X. Yang, H. Fisk, L.C. Wu, C. Hickey, J.C. Chandler, Y.Z.
- Wu, N.A. Heerema, K.K. Chan, D. Perrotti, J. Zhang, P. Porcu, F.K. Racke, R. Garzon, R.J. Lee, G.
- Marcucci, M.A. Caligiuri, Aberrant Overexpression of IL-15 Initiates Large Granular Lymphocyte
- Leukemia through Chromosomal Instability and DNA Hypermethylation, Cancer Cell. (2012).
- https://doi.org/10.1016/j.ccr.2012.09.009.
- 657 [27] M. Liu, W. Song, L. Huang, Drug delivery systems targeting tumor-associated fibroblasts for
- cancer immunotherapy, Cancer Lett. (2019). https://doi.org/10.1016/j.canlet.2019.01.032.
- 659 [28] W. Song, L. Shen, Y. Wang, Q. Liu, T.J. Goodwin, J. Li, O. Dorosheva, T. Liu, R. Liu, L. Huang,
- Synergistic and low adverse effect cancer immunotherapy by immunogenic chemotherapy and

- locally expressed PD-L1 trap, Nat. Commun. (2018). https://doi.org/10.1038/s41467-018-04605-x.
- 662 [29] H. Xu, M. Hu, M. Liu, S. An, K. Guan, M. Wang, L. Li, J. Zhang, J. Li, L. Huang, Nano-puerarin
- regulates tumor microenvironment and facilitates chemo- and immunotherapy in murine triple
- negative breast cancer model, Biomaterials. (2020).
- https://doi.org/10.1016/j.biomaterials.2020.119769.
- 666 [30] M. Liu, A.R. Khan, J. Ji, G. Lin, X. Zhao, G. Zhai, Crosslinked self-assembled nanoparticles for
- chemo-sonodynamic combination therapy favoring antitumor, antimetastasis management and
- 668 immune responses, J. Control. Release. (2018). https://doi.org/10.1016/j.jconrel.2018.10.007.
- 669 [31] G. Chen, A.C. Huang, W. Zhang, G. Zhang, M. Wu, W. Xu, Z. Yu, J. Yang, B. Wang, H. Sun, H.
- Kia, Q. Man, W. Zhong, L.F. Antelo, B. Wu, X. Xiong, X. Liu, L. Guan, T. Li, S. Liu, R. Yang, Y.
- Lu, L. Dong, S. McGettigan, R. Somasundaram, R. Radhakrishnan, G. Mills, Y. Lu, J. Kim, Y.H.
- Chen, H. Dong, Y. Zhao, G.C. Karakousis, T.C. Mitchell, L.M. Schuchter, M. Herlyn, E.J. Wherry,
- X. Xu, W. Guo, Exosomal PD-L1 contributes to immunosuppression and is associated with anti-
- PD-1 response, Nature. (2018). https://doi.org/10.1038/s41586-018-0392-8.
- 675 [32] X. Jiang, J. Wang, X. Deng, F. Xiong, J. Ge, B. Xiang, X. Wu, J. Ma, M. Zhou, X. Li, Y. Li, G. Li,
- W. Xiong, C. Guo, Z. Zeng, Role of the tumor microenvironment in PD-L1/PD-1-mediated tumor
- 677 immune escape, Mol. Cancer. (2019). https://doi.org/10.1186/s12943-018-0928-4.
- 678 [33] Y. Li, D.L. Hermanson, B.S. Moriarity, D.S. Kaufman, Human iPSC-Derived Natural Killer Cells
- Engineered with Chimeric Antigen Receptors Enhance Anti-tumor Activity, Cell Stem Cell. (2018).
- https://doi.org/10.1016/j.stem.2018.06.002.
- 681 [34] H. Seo, I. Jeon, B.S. Kim, M. Park, E.A. Bae, B. Song, C.H. Koh, K.S. Shin, I.K. Kim, K. Choi, T.
- Oh, J. Min, B.S. Min, Y.D. Han, S.J. Kang, S.J. Shin, Y. Chung, C.Y. Kang, IL-21-mediated
- reversal of NK cell exhaustion facilitates anti-Tumour immunity in MHC class I-deficient tumours,
- Nat. Commun. (2017). https://doi.org/10.1038/ncomms15776.
- 685 [35] S.J. Judge, W.J. Murphy, R.J. Canter, Characterizing the Dysfunctional NK Cell: Assessing the
- 686 Clinical Relevance of Exhaustion, Anergy, and Senescence, Front. Cell. Infect. Microbiol. (2020).
- https://doi.org/10.3389/fcimb.2020.00049.
- 688 [36] Q. Luo, J. V. Napoleon, X. Liu, B. Zhang, S. Zheng, P.S. Low, Targeted Rejuvenation of
- Exhausted Chimeric Antigen Receptor T-cells Regresses Refractory Solid Tumors, Mol. Cancer
- Res. (2022). https://doi.org/10.1158/1541-7786.mcr-21-0711.
- 691 [37] K. Tamada, D. Geng, Y. Sakoda, N. Bansal, R. Srivastava, Z. Li, E. Davila, Redirecting gene-
- 692 modified T cells toward various cancer types using tagged antibodies, Clin. Cancer Res. (2012).
- 693 https://doi.org/10.1158/1078-0432.CCR-12-1449.
- 694 [38] J.S.Y. Ma, J.Y. Kim, S.A. Kazane, S.H. Choi, H.Y. Yun, M.S. Kim, D.T. Rodgers, H.M. Pugh, O.
- Singer, S.B. Sun, B.R. Fonslow, J.N. Kochenderfer, T.M. Wright, P.G. Schultz, T.S. Young, C.H.
- Kim, Y. Cao, Versatile strategy for controlling the specificity and activity of engineered T cells,
- 697 Proc. Natl. Acad. Sci. U. S. A. (2016). https://doi.org/10.1073/pnas.1524193113.

- 698 [39] Y.G. Lee, H. Chu, Y. Lu, C.P. Leamon, M. Srinivasarao, K.S. Putt, P.S. Low, Regulation of CAR
- T cell-mediated cytokine release syndrome-like toxicity using low molecular weight adapters, Nat.
- 700 Commun. (2019). https://doi.org/10.1038/s41467-019-10565-7.
- 701 [40] Y.G. Lee, I. Marks, M. Srinivasarao, A.K. Kanduluru, S.M. Mahalingam, X. Liu, H. Chu, P.S. Low,
- 702 Use of a single CAR T cell and several bispecific adapters facilitates eradication of multiple
- antigenically different solid tumors, Cancer Res. (2019). https://doi.org/10.1158/0008-5472.CAN-
- 704 18-1834.
- 705 [41] H. Zhu, Y.S. Lai, Y. Li, R.H. Blum, D.S. Kaufman, Concise Review: Human Pluripotent Stem
- 706 Cells to Produce Cell-Based Cancer Immunotherapy, Stem Cells. (2018).
- 707 https://doi.org/10.1002/stem.2754.
- 708 [42] M. Carlsten, R.W. Childs, Genetic manipulation of NK cells for cancer immunotherapy:
- Techniques and clinical implications, Front. Immunol. (2015).
- 710 https://doi.org/10.3389/fimmu.2015.00266.
- 711 [43] D.A. Knorr, Z. Ni, D. Hermanson, M.K. Hexum, L. Bendzick, L.J.N. Cooper, D.A. Lee, D.S.
- Kaufman, Clinical-Scale Derivation of Natural Killer Cells From Human Pluripotent Stem Cells for
- 713 Cancer Therapy, Stem Cells Transl. Med. (2013). https://doi.org/10.5966/sctm.2012-0084.
- 714 [44] A.M. Martin, T.R. Nirschl, C.J. Nirschl, B.J. Francica, C.M. Kochel, A. Van Bokhoven, A.K.
- Meeker, M.S. Lucia, R.A. Anders, A.M. Demarzo, C.G. Drake, Paucity of PD-L1 expression in
- 716 prostate cancer: Innate and adaptive immune resistance, Prostate Cancer Prostatic Dis. (2015).
- 717 https://doi.org/10.1038/pcan.2015.39.
- 718 [45] Y. Kagoya, S. Tanaka, T. Guo, M. Anczurowski, C.H. Wang, K. Saso, M.O. Butler, M.D. Minden,
- N. Hirano, A novel chimeric antigen receptor containing a JAK-STAT signaling domain mediates
- superior antitumor effects, Nat. Med. (2018). https://doi.org/10.1038/nm.4478.
- 721 [46] Y. Chang, P.B. Hellwarth, L.N. Randolph, Y. Sun, Y. Xing, W. Zhu, X.L. Lian, X. Bao,
- 722 Fluorescent indicators for continuous and lineage-specific reporting of cell-cycle phases in human
- 723 pluripotent stem cells, Biotechnol. Bioeng. (2020). https://doi.org/10.1002/bit.27352.
- 724 [47] Y. Chang, R. Syahirah, S.N. Oprescu, X. Wang, J. Jung, S.H. Cooper, S. Torregrosa-Allen, B.D.
- 725 Elzey, A.Y. Hsu, L.N. Randolph, Y. Sun, S. Kuang, H.E. Broxmeyer, Q. Deng, X. Lian, X. Bao,
- 726 Chemically-defined generation of human hemogenic endothelium and definitive hematopoietic
- 727 progenitor cells, Biomaterials. 285 (2022) 121569.
- 728 https://doi.org/10.1016/J.BIOMATERIALS.2022.121569.
- 729 [48] Y. Chang, R. Syahirah, X. Wang, S. Toregrosa-Allen, B.D. Elzey, X. Lian, Q. Deng, H.E.
- 730 Broxmeyer, X. Bao, RESOURCE Engineering chimeric antigen receptor neutrophils from human
- 731 pluripotent stem cells for targeted cancer immunotherapy Running title: Generation of CAR-
- neutrophils from hPSCs, 2022.
- 733 [49] G. Roex, D. Campillo-Davo, D. Flumens, P.A.G. Shaw, L. Krekelbergh, H. De Reu, Z.N.
- Berneman, E. Lion, S. Anguille, Two for one: targeting BCMA and CD19 in B-cell malignancies

- 735 with off-the-shelf dual-CAR NK-92 cells, J. Transl. Med. (2022). https://doi.org/10.1186/s12967-
- 736 022-03326-6.
- 737 [50] T. Ingegnere, F.R. Mariotti, A. Pelosi, C. Quintarelli, B. De Angelis, N. Tumino, F. Besi, C.
- 738 Cantoni, F. Locatelli, P. Vacca, L. Moretta, Human CAR NK cells: A new non-viral method
- 739 allowing high efficient transfection and strong tumor cell killing, Front. Immunol. (2019).
- 740 https://doi.org/10.3389/fimmu.2019.00957.
- 741 [51] E. Liu, D. Marin, P. Banerjee, H.A. Macapinlac, P. Thompson, R. Basar, L. Nassif Kerbauy, B.
- Overman, P. Thall, M. Kaplan, V. Nandivada, I. Kaur, A. Nunez Cortes, K. Cao, M. Daher, C.
- Hosing, E.N. Cohen, P. Kebriaei, R. Mehta, S. Neelapu, Y. Nieto, M. Wang, W. Wierda, M.
- Keating, R. Champlin, E.J. Shpall, K. Rezvani, Use of CAR-Transduced Natural Killer Cells in
- 745 CD19-Positive Lymphoid Tumors, N. Engl. J. Med. (2020).
- 746 https://doi.org/10.1056/nejmoa1910607.
- 747 [52] Y. Liu, Y. Zhou, K.H. Huang, X. Fang, Y. Li, F. Wang, L. An, Q. Chen, Y. Zhang, A. Shi, S. Yu, J.
- Zhang, Targeting epidermal growth factor-overexpressing triple-negative breast cancer by natural
- 749 killer cells expressing a specific chimeric antigen receptor, Cell Prolif. (2020).
- 750 https://doi.org/10.1111/cpr.12858.
- 751 [53] X. Chen, J. Han, J. Chu, L. Zhang, J. Zhang, C. Chen, L. Chen, Y. Wang, H. Wang, L. Yi, J.B.
- 752 Elder, Q.E. Wang, X. He, B. Kaur, E.A. Chiocca, J. Yu, A combinational therapy of EGFR-CAR
- NK cells and oncolytic herpes simplex virus 1 for breast cancer brain metastases, Oncotarget.
- 754 (2016). https://doi.org/10.18632/oncotarget.8526.
- 755 [54] C. Zhang, M.C. Burger, L. Jennewein, S. Genßler, K. Schönfeld, P. Zeiner, E. Hattingen, P.N.
- Harter, M. Mittelbronn, T. Tonn, J.P. Steinbach, W.S. Wels, ErbB2/HER2-Specific NK Cells for
- Targeted Therapy of Glioblastoma, J. Natl. Cancer Inst. (2016). https://doi.org/10.1093/jnci/djv375.
- 758 [55] I.M. Montagner, A. Penna, G. Fracasso, D. Carpanese, A. Dalla Pietà, V. Barbieri, G. Zuccolotto,
- A. Rosato, Anti-PSMA CAR-engineered NK-92 Cells: An Off-the-shelf Cell Therapy for Prostate
- 760 Cancer, Cells. (2020). https://doi.org/10.3390/cells9061382.
- 761 [56] A. Nellan, D.W. Lee, Paving the road ahead for CD19 CAR T-cell therapy, Curr. Opin. Hematol.
- 762 (2015). https://doi.org/10.1097/MOH.000000000000182.
- 763 [57] Y. Robbins, S. Greene, J. Friedman, P.E. Clavijo, C. Van Waes, K.P. Fabian, M.R. Padget, H.A.
- Sater, J.H. Lee, P. Soon-Shiong, J. Gulley, J. Schlom, J.W. Hodge, C.T. Allen, Tumor control via
- targeting pd-11 with chimeric antigen receptor modified nk cells, Elife. (2020).
- 766 https://doi.org/10.7554/eLife.54854.
- 767 [58] K.P. Fabian, M.R. Padget, R.N. Donahue, K. Solocinski, Y. Robbins, C.T. Allen, J.H. Lee, S.
- 768 Rabizadeh, P. Soon-Shiong, J. Schlom, J.W. Hodge, PD-L1 targeting high-affinity NK (t-haNK)
- cells induce direct antitumor effects and target suppressive MDSC populations, J. Immunother.
- 770 Cancer. (2020). https://doi.org/10.1136/jitc-2019-000450.
- 771 [59] S.D. Reighard, S.A. Cranert, K.M. Rangel, A. Ali, I.E. Gyurova, A.T. de la Cruz-Lynch, J.A.

- Tuazon, M. V. Khodoun, L.C. Kottyan, D.F. Smith, H.I. Brunner, S.N. Waggoner, Therapeutic
- 773 Targeting of Follicular T Cells with Chimeric Antigen Receptor-Expressing Natural Killer Cells,
- 774 Cell Reports Med. (2020). https://doi.org/10.1016/j.xcrm.2020.100003.
- 775 [60] F. Zhang, H. Wei, X. Wang, Y. Bai, P. Wang, J. Wu, X. Jiang, Y. Wang, H. Cai, T. Xu, A. Zhou,
- Structural basis of a novel PD-L1 nanobody for immune checkpoint blockade, Cell Discov. (2017).
- 777 https://doi.org/10.1038/celldisc.2017.4.
- 778 [61] Y. Zhang, D.L. Wallace, C.M. De Lara, H. Ghattas, B. Asquith, A. Worth, G.E. Griffin, G.P.
- Taylor, D.F. Tough, P.C.L. Beverley, D.C. Macallan, In vivo kinetics of human natural killer cells:
- The effects of ageing and acute and chronic viral infection, Immunology. (2007).
- 781 https://doi.org/10.1111/j.1365-2567.2007.02573.x.
- 782 [62] J.C. Sun, J.N. Beilke, N.A. Bezman, L.L. Lanier, Homeostatic proliferation generates long-lived
- natural killer cells that respond against viral infection, J. Exp. Med. (2011).
- 784 https://doi.org/10.1084/jem.20100479.
- 785 [63] B. Foley, S. Cooley, M.R. Verneris, J. Curtsinger, X. Luo, E.K. Waller, C. Anasetti, D. Weisdorf,
- J.S. Miller, Human Cytomegalovirus (CMV)-Induced Memory-like NKG2C + NK Cells Are
- 787 Transplantable and Expand In Vivo in Response to Recipient CMV Antigen, J. Immunol. (2012).
- 788 https://doi.org/10.4049/jimmunol.1201964.
- 789 [64] S. Paust, H.S. Gill, B.Z. Wang, M.P. Flynn, E.A. Moseman, B. Senman, M. Szczepanik, A. Telenti,
- 790 P.W. Askenase, R.W. Compans, U.H. Von Andrian, Critical role for the chemokine receptor
- 791 CXCR6 in NK cell-mediated antigen-specific memory of haptens and viruses, Nat. Immunol.
- 792 (2010). https://doi.org/10.1038/ni.1953.
- 793 [65] V. Hoyos, B. Savoldo, C. Quintarelli, A. Mahendravada, M. Zhang, J. Vera, H.E. Heslop, C.M.
- 794 Rooney, M.K. Brenner, G. Dotti, Engineering CD19-specific T lymphocytes with interleukin-15
- and a suicide gene to enhance their anti-lymphoma/leukemia effects and safety, Leukemia. (2010).
- 796 https://doi.org/10.1038/leu.2010.75.
- 797 [66] M.T. Kasaian, M.J. Whitters, L.L. Carter, L.D. Lowe, J.M. Jussif, B. Deng, K.A. Johnson, J.A.S.
- 798 Witek, M. Senices, R.F. Konz, A.L. Wurster, D.D. Donaldson, M. Collins, D.A. Young, M.J.
- Grusby, IL-21 limits NK cell responses and promotes antigen-specific T cell activation: A mediator
- of the transition from innate to adaptive immunity, Immunity. (2002).
- 801 https://doi.org/10.1016/S1074-7613(02)00295-9.
- 802 [67] S. Venkatasubramanian, S. Cheekatla, P. Paidipally, D. Tripathi, E. Welch, A.R. Tvinnereim, R.
- 803 Nurieva, R. Vankayalapati, IL-21-dependent expansion of memory-like NK cells enhances
- protective immune responses against Mycobacterium tuberculosis, Mucosal Immunol. (2017).
- https://doi.org/10.1038/mi.2016.105.
- 806 [68] M. Granzin, A. Stojanovic, M. Miller, R. Childs, V. Huppert, A. Cerwenka, Highly efficient IL-21
- and feeder cell-driven ex vivo expansion of human NK cells with therapeutic activity in a xenograft
- mouse model of melanoma, Oncoimmunology. (2016).

809		https://doi.org/10.1080/2162402X.2016.1219007.
810	[69]	A. Biederstädt, K. Rezvani, Engineering the next generation of CAR-NK immunotherapies, Int. J.
811		Hematol. (2021). https://doi.org/10.1007/s12185-021-03209-4.
812	[70]	F. Kandarian, G.M. Sunga, D. Arango-Saenz, M. Rossetti, A flow cytometry-based cytotoxicity
813		assay for the assessment of human NK cell activity, J. Vis. Exp. 2017 (2017).
814		https://doi.org/10.3791/56191.
815		
816		
817		